Experimental investigation of the effect of scale-up on mixing efficiency in oscillatory flow baffled reactors (OFBR) using principal component based image analysis as a novel noninvasive residence time distribution measurement approach

Joesph A. Oliva*, Kanjakha Pal*, Alastair Barton**, Paul Firth**, and Zoltan K. Nagy*

*School of Chemical Engineering, Purdue University, West Lafayette, IN 47907, US
**Alconbury Weston Ltd, Stoke-on-Trent, ST4 3PE, United Kingdom

Abstract

Oscillatory flow strategies through baffled tubular reactors provide an efficient approach in improving process kinetics through enhanced micromixing and heat transfer. Known to have high surface area to volume ratios, oscillatory flow baffled reactors (OFBR) generate turbulence by superimposing piston driven oscillatory flow onto the net flow generated by a pump. By tuning the oscillating parameters (amplitude and frequency), one can tailor the residence time distribution of the system for a variety of multiphase applications. Using a microscope camera, principal component image analysis, and pulse tracer injections, a novel noncontact approach has been developed to experimentally estimate dispersion coefficients in two geometrically different systems (DN6 and DN15, Alconbury Weston Ltd.). The paper also introduces for the first time a novel scaled-down version of the commercially available DN15 OFBR, the DN6 (about 10 times smaller scale), and provides a comprehensive experimental investigation of the effect of oscillation parameters on the residence time distributions (RTD) in both systems. The oscillation amplitude was found to have a significant positive correlation with the dispersion coefficient with 1 mm providing the least amount of dispersion in either system. Oscillation frequency had a less significant impact on the dispersion coefficient, but optimal operation was found to occur at 1.5 Hz for the DN6 and 1.0Hz for the DN15. Until now, OFBR literature has not distinguished between piston and pump driven flow. Pump driven flow was found to be ideal for both systems as it minimizes the measured dispersion coefficient. However, piston driven turbulence is essential for avoiding particle settling in two phase (solid-liquid) systems and should be considered in applications like crystallization.

Keywords: residence time distribution, oscillatory flow, continuous reactions

Introduction

Increasingly popular for both synthesis and purification applications, continuous oscillatory flow strategies improve process kinetics through enhanced micromixing and heat transfer characteristics.[1] Specifically useful for dual phase systems (liquid- liquid/ solid- liquid), oscillatory flow baffled reactors (OFBR) offer process flexibility with adaptable configurations. OFBRs are often divided into several zones which allow for the implementation of temperature profiles and the spatial distribution of reagents across multiple injection points[1]. These added degrees of freedom provide numerous design advantages when compared to their continuous stirred tank counterparts.

Compared to traditional plug flow reactors (PFRs), OFBRs generate turbulence by superimposing an oscillatory flow onto the net flow through the use of a piston. By imposing this oscillatory turbulence, OFBRs do not need to operate at high throughput flow rates like PFRs, meaning smaller tube lengths and holdup volumes. However, several authors have indicated that these oscillations have a significant impact on the RTD of the system,[2,4,5,6] but do not consider system geometry or scale up. Herein, two commercial systems of different geometry and scale will be evaluated under a variety of operating conditions.

OFBR Model	D (mm)	d_o (mm)	l_b (mm)	Glass Thickness (mm)	Volume (mL)
DN6	6.85	3.5	11	3	37.5
DN15	15	7.5	21.4	2	312.5

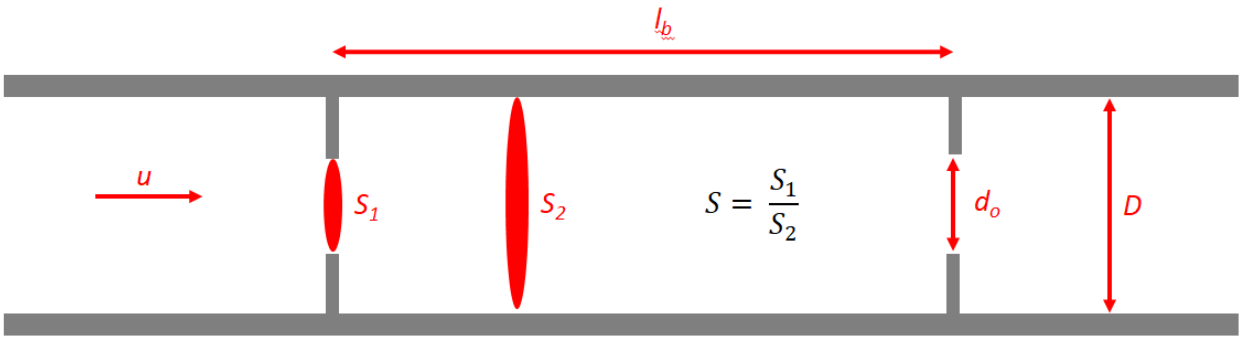

Figure 1. Illustration of OFBC geometry. Adapted from McDonough[7]

Conventional oscillatory baffled reactors vary in geometry and have diameters of 15 mm or greater,[7] while the newer (more recent) mesoscale reactors have diameters in the range of 4-5 mm. Regardless of scale, the commercial application of oscillatory systems are generally limited to purely liquid systems, as plug flow operation in a two phase (solid/liquid) system is still mainly a topic of interest amongst academics, especially for shear-sensitive applications.[8]

The flow characteristics in oscillatory systems are largely governed by both operating and geometric parameters.[9] As described in Figure 1, *S* controls the size and shape of eddies formed, while adequate distance between baffles (l_b) ensures fully developed vortices and the minimization of mixing dead zones.[10,11] Baffle type also plays a major role and should be chosen appropriately for a given application. For example, a major concern in designing crystallization systems is minimizing shear stress, as it can lead to crystal breakage and broad size distributions.[12] Integral baffles (like those in the DN6 and DN15) provide a low shear environment[13,14] by smoothly constricting the inner diameter of the tube periodically, making them ideal for these applications.

Four dimensionless parameters define the fluid flow patterns in an OBC, that is, the oscillatory Reynolds number (Re_o), the net flow Reynolds number (Re_n), the Strouhal number (St), and ψ, the ratio of oscillatory and net flows.

$$Re_o = \frac{2\pi f x_0 \rho D}{\mu} \quad (1)$$

$$Re_n = \frac{\rho u D}{\mu} \quad (2)$$

$$St = \frac{D}{4\pi x_0} \quad (3)$$

$$\psi = \frac{Re_o}{Re_n} \quad (4)$$

Note: x_0 is the piston amplitude, ρ is the solution density, D is the diameter of the tube segment, u is the mean superficial velocity and μ is the solution viscosity. The St measures effective eddy

propagation by simply taking the ratio of the column diameter to piston stroke length[6]. The Re_o represents the turbulence generated by the oscillating piston. Similar to traditional fluid dynamics, the Re_n is a ratio of inertial to viscous forces. The ratio of oscillatory and net flow Re result in the overall mixing parameter ψ, a commonly used turbulence parameter.

Residence Time Distributions in Oscillatory Baffled Systems

Table 1. Optimum operating parameters of OFBRs in literature

System	DN15	Custom	Custom	Amicon-Wright
Length (m)	~5	5	20.5	0.67
Inner Diameter (mm)	15	25	40	23
Vertical (V) or Horizontal (H)	V	V	V	H
Re_o	94-3,000	435	2008	Not reported
Optimal Frequency (Hz)	Both high (5) and low (1)	Not reported	2	No effect
Optimal Amplitude (mm)	1	Not reported	4	1
Conclusions	Ψ is not sufficient in characterizing a system	Scale up can be achieved using a multi-tube configuration	Increasing x_0 led to increasing dispersion	Frequency had an insignificant effect on dispersion measurements
Author	Kacker[4]	Ni[15]	Pereira[6]	Dickens[16]

A major advantage in oscillatory tubular systems is the ability to operate near plug flow for narrow residence time distributions[17]. As seen in Table 1, several authors have worked to develop the operating framework for continuous oscillatory baffled systems. Each had a geometrically different system, but the trends for optimal operation are similar. Kacker's work used the commercially available DN15 manufactured by Alconbury Weston Ltd. He found that Ψ is not a sufficient parameter in characterizing the fluid dynamics of their system and that optimal operation occurred at both high and low frequencies as long as the amplitude remained small (1 mm). Similarly, Dickens reported the same optimal amplitude of oscillation and that frequency had little to no effect on dispersion measurements. Moreover, both Kacker's and Dickens' results agree with those conducted by Pereira, who showed that increasing the amplitude of oscillation resulted in increased dispersion and a larger mean residence time. Ni used flow visualization

studies to evaluate the benefits of both baffles and oscillations in achieving plug flow behavior at minimal flow rates (Re_N). Plug flow operation is vital for crystallization, as narrow CSDs are directly proportional to narrow RTDs. Moreover, the majority of RTDs in OFBR literature are conducted for single phase liquid systems, which do not accurately represent solid-liquid systems. Kacker, however, performed both liquid and solid-liquid RTD studies and showed that plug flow operation is achievable under a variety of conditions.

Mean Residence Time and Dispersion Calculations

To evaluate the residence time distributions at different flow conditions, both mean residence time and dispersion calculations are often used:[4,5]

$$t_{mean} = \frac{\int_0^\infty t*c\ dt}{\int_0^\infty c\ dt} \tag{5}$$

$$\sigma^2 = \frac{\int_0^\infty (t-t_{mean})^2*c\ dt}{\int_0^\infty c\ dt} \tag{6}$$

$$\frac{\sigma^2}{t_{mean}^2} = 2\left(\frac{\mathcal{D}}{uL}\right) + 8\left(\frac{\mathcal{D}}{uL}\right)^2 \tag{7}$$

where t is time (s), c is the concentration (mg/mL), σ is the variance, $\mathcal{D}$ (m^2/s) is the dispersion coefficient, u (m/s) is the net flow superficial velocity, and L (m) is the distance between the tracer's injection point and the point at which the concentration measurement is taken. While equations (5) and (6) are standard in the RTD literature, Levenspiel[18] solved the dispersion model subject to the open-open boundary condition to obtain the analytical solution found in equation (7). Using this method, Kacker experimentally determined $\mathcal{D}/(uL)$ values for the commercially available DN15 to be on the order of 10^{-2}. These results should be independent of scale, as equations (5) – (7) are independent of geometrical considerations.

One limitation of the proposed approach in determining the dispersion coefficient is that equations (5) and (6) only consider the area under the concentration versus time curve, while

information regarding the shape of the curve is lost. To better consider this lumped information, an asymmetry factor was introduced.

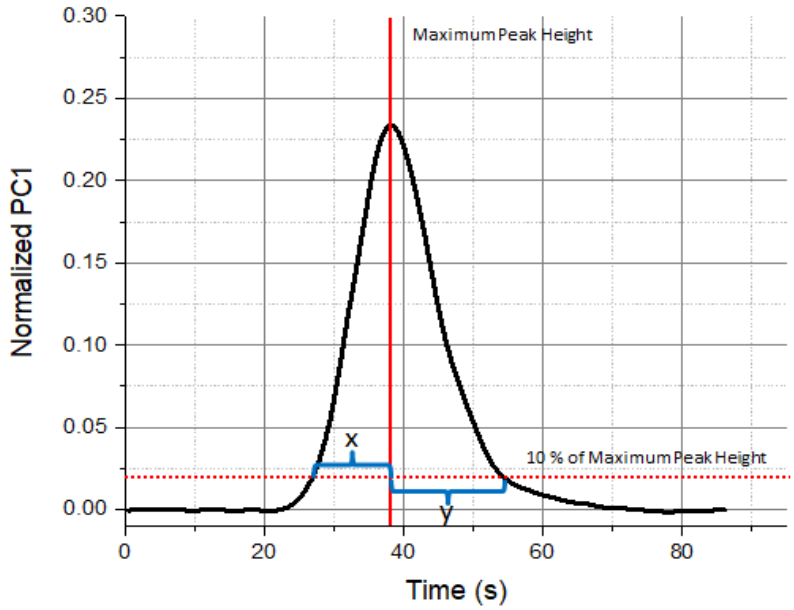

Figure 2. Asymmetry factor illustration

$$Asymmetry\ Factor = \frac{y}{x} \tag{8}$$

Typically used to describe qualitative information in chromatographs,[19] the asymmetry factor provides an additional means of comparing RTDs under different process conditions. Peak "tailing" is not adequately described by dispersion calculations because the area under the peak tail is rather small. Asymmetry factors close to 1 indicate minimal peak tailing, while factors much larger than 1 give insight regarding the amount of back mixing (tracer spreading in the reverse direction) caused by piston drawback. All in all, the asymmetry factor is a supplementary tool that should be used in combination with the dispersion coefficient to evaluate overall system performance.

Principal Component Image Analysis (PCA)

Principal component transformations are an advanced technique that reduces the dimensionality of a dataset, such that correlations found within the data are measured as a maximization of uncorrelated variations.[20,21] Specific to image analysis applications, PCA is a linear orthogonal transformation that converts traditional RGB measurement space to PC1-PC3 space. PC1 is a maximization of the statistical variance (σ) in the RGB data set. Each subsequent PC also maximizes the statistical variance, subject to the constraint that it is orthogonal to the previous principal components. In this way, the signal is largely captured in PC1 and is weaker with each additional principal component. The utility of this approach is that a single measurement can be tracked with time (PC1) and is directly proportional to the concentration of tracer in the system. This technique is often used to define a new basis set of vectors (viz. the first three principal components) and has many commercial applications.

In regards to the following residence time distribution studies, PCA is used to identify the presence of methylene blue as a pulse tracer. Although nontraditional for this application, this technique has novel capabilities compared to traditional concentration measurements with UV probes. In this oscillatory system, probe-based measurement ports can only be located at the elbow/tube junctions in order to avoid interference with the baffles. However, the dispersion term in the elbow is likely different than that found in the tube segment, creating a parameter mismatch at the point of measurement.[22] In using a microscope camera measurement, with PCA image analysis, a novel approach was developed that measures RTDs and dispersion coefficients at different geometrical locations without direct contact in the system.

Simply using RGB camera measurements without the processing of PCA is ineffective at determining RTDs, since the proportionality of G/B changes nonlinearly with the concentration seen by the camera. In other words, a difficult calibration is required to correlate RGB intensity

measurements with methylene blue concentrations. Grayscale video processing is a potential RGB alternative for RTD measurements. Although appropriate for OFBR RTD studies, grayscale video processing is sensitive to process lighting conditions and camera positioning. PCA, however, measures uncorrelated variations in the dataset, which is independent of the absolute intensity measured by the camera. That is, if the unprocessed measurements from an experiment fall in the upper range of the 256 bit scale on one day but fall in a lower range on a different day, the two experiments can still be compared because the first principal component measurements are with respect to changes in the statistical variance and not the absolute measurement! Therefore, by tracking changes in variance instead of changes in the true measurement, PCA is a more robust and appropriate processing method.

Materials and Methods

Residence Time Distribution Studies

The first set of experiments implemented the newly designed Nitech DN6 (Alconbury Weston Ltd) OFBR with a total holdup volume of 37.5 mL distributed across 2 equal tube segments and a single elbow connection, while the second set utilized a Nitech DN15 (Alconbury Weston Ltd) with a holdup of 312.5 mL (roughly one order of magnitude difference in scale). Methylene blue (Lab grade ≥99.5% purity, Fisher Scientific) was injected as a pulse tracer (380 μg/mL) using a syringe pump (kd Scientific, Infusion). Water was pumped at the inlet using a peristaltic pump (MasterFlex L/S, Cole-Palmer) at varying flow rates. The entire system was jacketed and held at 25 ℃ for the duration of the experiment. A Firefly Pro microscope camera (RW180) was used to record video images at 720×480 resolution at 15 fps.

In order to relate the DN6 system parameters with the DN15, several decisions were made regarding the injection volume of methylene blue and the flow rate of the bulk fluid (water). Using the cross sectional area of the DN6 and a set water flow rate of 15 mL/min, an estimated axial velocity was determined. This estimated axial velocity was kept constant and was directly translated to the DN15 and the equivalent water flow rate was determined to be 154.7 mL/min. In regards to the pulse tracer injection, the original intention was to scale the methylene blue volume with the total holdup of each system. However, due to limitations on the injection speed of the syringe pump (max 52 mL/min), it was determined that the larger volume required for the DN15 could not be injected at a quick enough rate to be considered instantaneous. As a result, the injection speed between the systems was kept constant and the maximum injection volume for that speed was used in the DN15 experiments. The final injection parameters are as follows: 0.2 mL at 40 mL/min for the DN6 and 0.25 mL at 50 mL/min for the DN15.

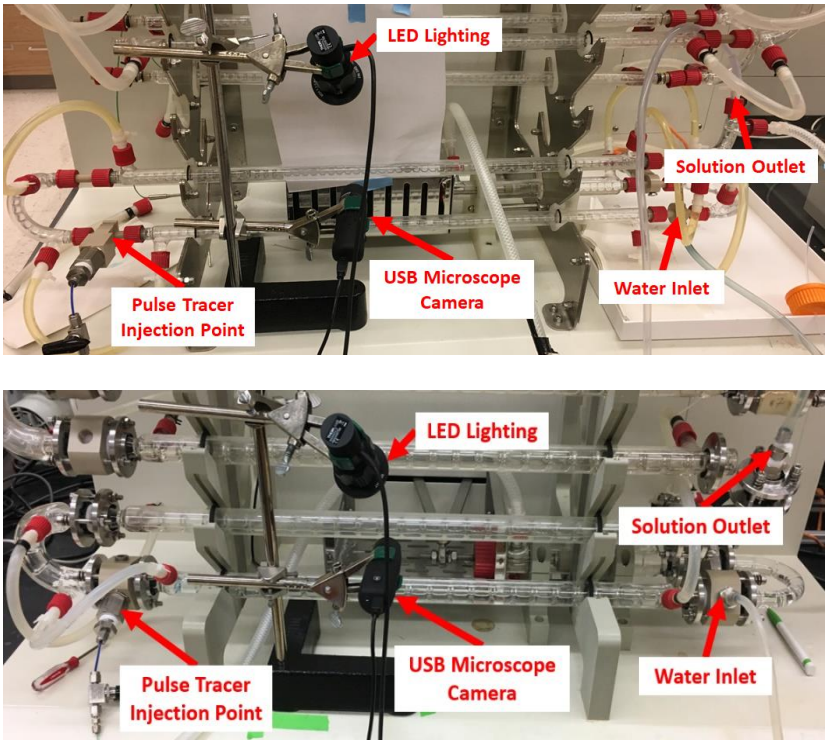

Figure 3. Pictures with main components of the DN6 (top) and DN15 (bottom) RTD experimental setup

Prior to the application of PCA, the dataset is averaged to 1 fps in order to reduce noise in the RGB intensity measurements. Moreover, this technique helps to maximize the variations found in PC1 by avoiding large noise spikes that result from air travelling through the system. The goal of this approach is to completely capture the variations of the system in PC1 instead of a combination of all three PCs. The developed Matlab software identifies the initial pulse tracer by taking the derivative of the first principal component. When the derivative of the first component exceeds a sufficiently large value, the software checks subsequent local points to ensure pulse tracer detection. This approach limits noisy data and ensures proper pulse tracer detection limits. The end detection limit utilizes a baseline averaging technique. A baseline is defined as an average of the final 25% of data points. When the principal component measurement crosses this baseline, an endpoint limit is defined. Herein, the width of the RTD is defined as the difference in time

between the initial tracer pulse detection limit and the endpoint tracer limit. To normalize the distribution, a min-max difference is used.

$$PC1_{max} = max^{90}\left\{\begin{pmatrix} PC1_{1,1} & \cdots & PC1_{1,m} \\ \vdots & \ddots & \vdots \\ PC1_{n,1} & \cdots & PC1_{n,m} \end{pmatrix}\right\} \quad (9)$$

$$PC1_{min} = min^{10}\left\{\begin{pmatrix} PC1_{1,1} & \cdots & PC1_{1,m} \\ \vdots & \ddots & \vdots \\ PC1_{n,1} & \cdots & PC1_{n,m} \end{pmatrix}\right\} \quad (10)$$

$$Normalized\ PC1 = \frac{PC1_{max} - PC1_{min}}{PC1_{max}} \quad (11)$$

That is, the 90th percentile (90% of the data falls below this point) is used as the max while the 10th percentile is used as the min. The difference between the max and min is taken and divided by the max for each frame. Note that this is the approach used to reduce the two dimensional data matrix measured for each frame to a single scalar value. Herein, these are the scalar values tracked with time and reported in the RTD results section.

Limits of Detection using PCA and Methylene Blue

In using a non-contact microscope camera instead of a UV-vis probe for concentration measurements, the limit of detection may come into question as it relates to the accuracy of the dispersion coefficient calculations. To measure the limit of detection, a series of step changes were implemented before reaching a controlled state of operation. In other words, several known concentrations of methylene blue were pumped through the inlet and held for several minutes before the subsequent step change was implemented. Firstly, water was introduced to the system, followed by dilute methylene blue at 0.95 µM, 0.71 µM, 0.48 µM 0.24 µM, and 0.12 µM, respectively. When the measure of principal component 2 dips below that measured for water, the limit of detection is reached. Note that PC2 is used here instead of PC1 because at this dilution, the variations measured in PC1 for each concentration are very similar to that of water. However,

the subtle variations in the dataset are completely captured by PC2. Using the aforementioned method, the limit of detection was determined to be 0.24 μM, thus validating the use of a microscope camera and PCA as an RTD measurement approach.

Results and Discussion

Summary of Experimental Conditions

Table 3. DN6 (top) and DN15 (bottom) RTD experiments and dispersion calculation results

Exp.	Flow Rate (mL/min)	x_0 (mm)	f (Hz)	Re_o	ψ	Asymmetry Factor	$\frac{\mathcal{D}}{uL}$
1	15	1	1	48.2	0.9	1.6	0.017
2	15	3	1	144.6	2.8	1.7	0.019
3	15	5	1	241.1	4.6	1.6	0.022
4	15	10	1	482.2	9.3	2.0	0.042
5	15	1	0.2	9.6	0.2	1.9	0.027
6	15	1	1.5	72.3	1.4	1.4	0.015
7	15	1	3	144.6	2.8	1.8	0.034
8	10	1	1	48.2	1.4	2.2	0.023
9	30	1	1	48.2	0.5	2.5	0.014

Exp.	Flow Rate (mL/min)	x_0 (mm)	f (Hz)	Re_o	ψ	Asymmetry Factor	$\frac{\mathcal{D}}{uL}$
1	154.7	1	1	112.6	0.5	1.5	0.010
2	154.7	3	1	337.9	1.5	1.4	0.012
3	154.7	5	1	563.1	2.4	1.5	0.020
4	154.7	10	1	1126.2	4.9	2.0	0.034
5	154.7	1	0.2	168.9	0.7	1.4	0.015
6	154.7	1	1.5	337.9	1.5	2.2	0.023
7	154.7	1	3	22.5	0.1	1.6	0.014
8	15	1	1	112.6	5.1	1.7	0.018
9	38.7	1	1	112.6	2.0	1.5	0.017
10	77.4	1	1	112.6	1.0	1.7	0.015

Changes in Amplitude

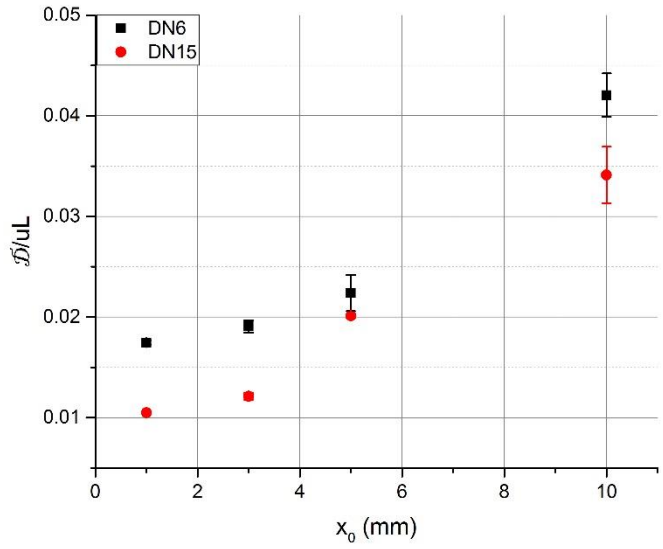

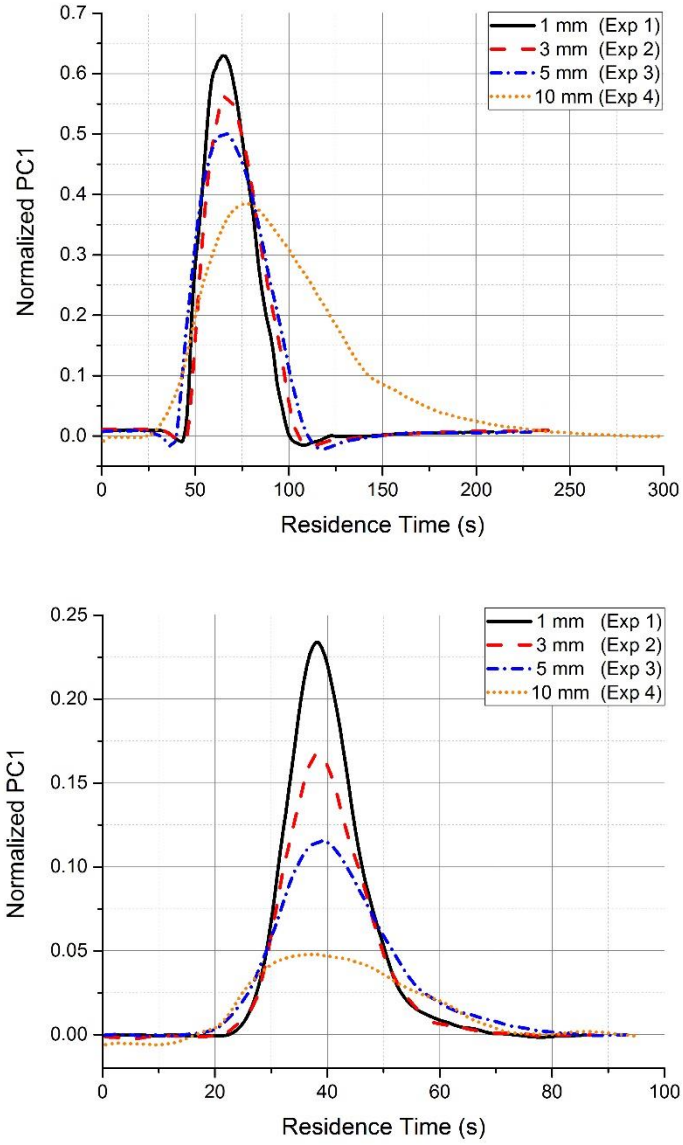

Figure 4. (top) Measured dispersion coefficients over a range of piston amplitudes (middle) RTDs in the DN6 (bottom) RTDs in the DN15

As the amplitude of the piston increases, the width of the RTD broadens and the dispersion coefficient increases. The stroke length of the piston directly influences the RTD because a longer drawback leads to more back mixing and inherent deviation from plug flow operation. Similarly, large amplitudes can lead to the fluid passing through multiple baffles, leading to additional non-idealities in flow behavior. Note that these results are in line with those found by Kacker and

Mackley in that operating at minimal amplitude leads to the lowest dispersion coefficient. Although minimal dispersion leads to "plug flow" behavior, one must also consider the minimal energy required to maintain solid suspension in two phase applications like crystallization. Solid suspension is essential to prevent system clogging and particle settling. With respect to process design, one must choose appropriate piston conditions keeping in mind the direct proportionality of the solid's settling velocity to both the size and true density of the crystal.[23]

Changes in Frequency

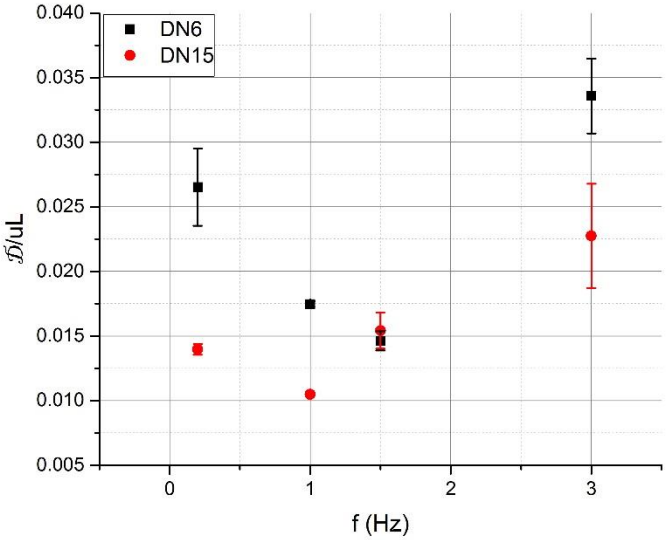

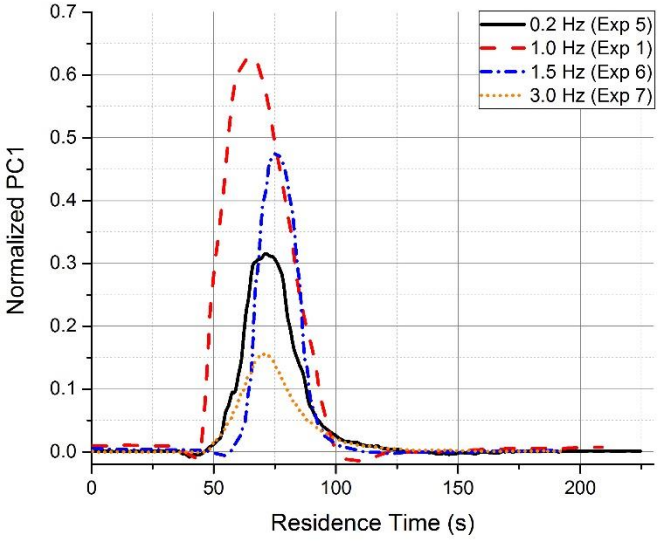

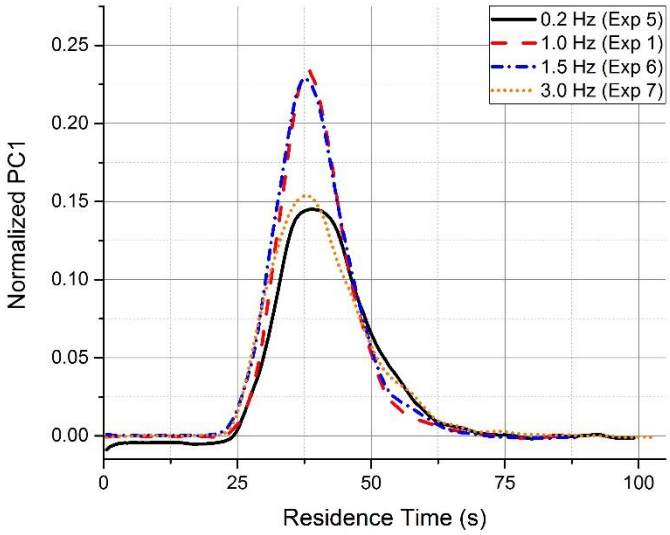

Figure 5. (top) Measured dispersion coefficients over a range of piston frequencies (middle) RTDs in the DN6 (bottom) RTDs in the DN15

Similar to the results shown by Dickens, varying the frequency of the piston had an uncorrelated effect on the dispersion experienced by the system. Optimal operation was found to be at 1.5 Hz for the DN6 and 1.0 Hz for the DN15 when the amplitude was constant at 1 mm. Both high and low frequency operation saw more of a 'tailing effect' on the residence time distribution and this may be insightful in describing vortex propagation for the given baffle geometries. Because frequency seems to have an effect on the shape of the RTD, changing the frequency of the forward vs backwards plunges may be of interest. This operating strategy gives rise to the idea that asymmetrical oscillations could minimize dispersion such that plug flow operation is achievable at a variety of operating conditions and may be important for solid suspension applications.

System Sensitivity to Flow Type

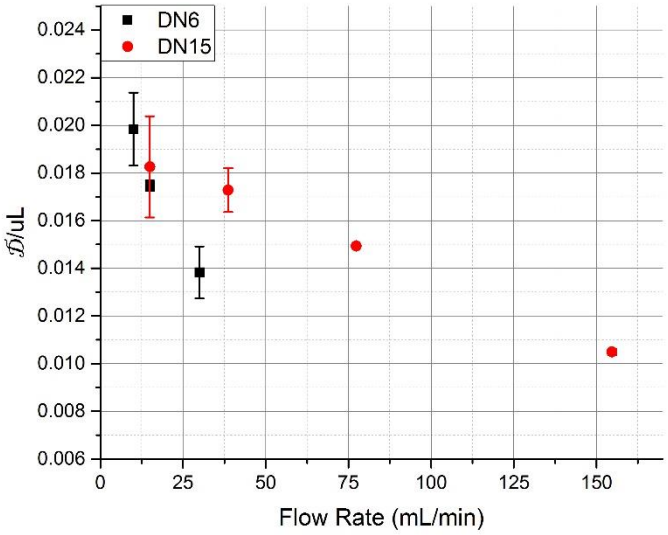

Figure 6. Measured dispersion coefficients at different pump flow rates

Over the range of flow rates in this study, the dispersion coefficient decreases as the pump induced flow rate increases under constant piston conditions. Higher flow rates clear the pulse tracer faster and are less affected by the oscillations of the piston. That is, piston oscillations generate substantial back mixing as previously described in the amplitude analysis section of the results. Again, there exists a trade-off between minimizing dispersion and generating turbulence. One of the advantages of an oscillatory flow strategy is decreased system length as compared to the traditional PFR. Unrealistically long lengths are often required in PFR systems to generate the turbulence required for solid suspension. By superimposing oscillations onto the net flow, OFBRs generate similar turbulent conditions, but at lower flow rates with the tradeoff being increased dispersion in the system.

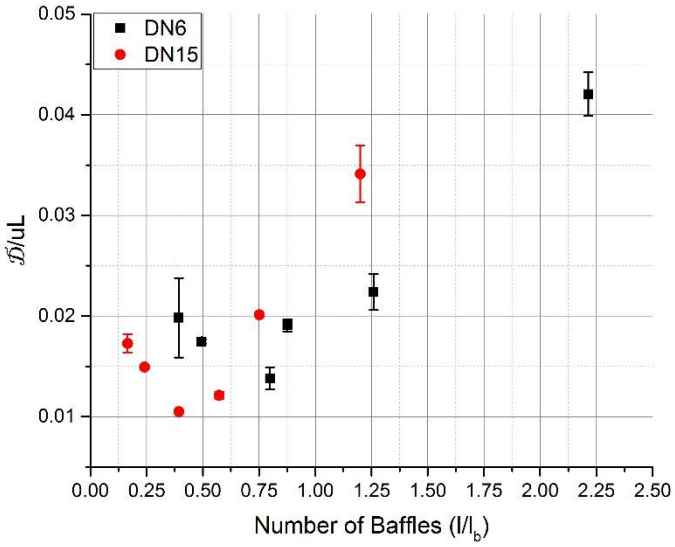

Figure 7. Measured dispersion as the fluid flows through a set number of baffles per second

In order to properly address optimal operating strategies for both OFBC systems, one must consider how far the fluid is travelling with each stroke of the piston. Initial intuition would lead one to consider how dispersion changes as a result of how much volume is pushed through a baffle with a single forward piston stroke. While adequate for describing a single system, this reasoning does not address the different diameters of each OFBR. In other words, because both S and l_b vary between the two systems, comparing volume equivalents is insufficient in describing the "spreading" of the pulse tracer. A more appropriate means of evaluation is to compare the axial distances travelled by the pulse tracer with l_b.

Figure 7 describes how dispersion changes as the axial net flow of the fluid traverses multiple baffles. Oddly enough, both OFBR systems exhibit a minimum dispersion coefficient at some pivot point (roughly 0.8 for the DN6 and 0.4 for the DN15). As the fluid gets pushed past multiple baffles, the dispersion coefficient drastically increases. However, when the fluid does not travel a far enough axial distance, the dispersion also increases, which seems perplexing.

This phenomenon gives rise to distinguishing between two types of flow regimes: pump dominated and piston dominated flow.

The mechanism by which fluid flows through the OFBR can be broken down into two parts: axial flow generated by the forward stroke of the piston and axial flow generated by the peristaltic pump. Piston generated flow can be approximated by dividing the volume of fluid displaced by the piston each second by the cross sectional area of the tube. Pump generated flow is approximated by dividing the volumetric flow rate of the pump by the cross sectional area of the tube. Using these approximations along with equation (12), piston and pump dominated flow regions are defined in Figure 8.

$$Piston\ to\ Total\ Ratio = \frac{Axial\ Piston\ Flow}{Axial\ Piston\ Flow + Axial\ Pump\ Flow} \tag{12}$$

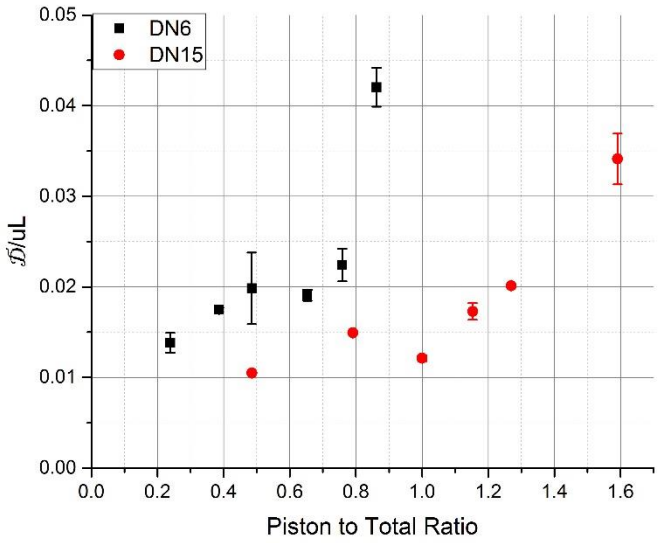

Figure 8.Measured dispersion while operating in either piston or pump dominated flow

Figure (8) transforms the data in Figure (7) into a more appropriate treatment of system parameters. By distinguishing the mechanisms by which fluid is being axially transferred, the relationship between dispersion and flow becomes quite apparent. In piston dominated flow

(Ratios > ~0.75 in the DN6 and Ratios >~1.0 in the DN15), the dispersion coefficient grows rapidly because the superimposed oscillations largely affect the net flow generated by the pump. In pump dominated flow, system dispersion is lower and therefore ideal for operation. In operating a two phase system, one would want to design process parameters such that the system is operating in pump dominated flow while tailoring the oscillations to ensure proper solid suspension. Together, pump driven flow and controlled oscillations allow for narrow residence time distributions which directly correlate to narrow crystal size distributions (CSDs) for a variety of pharmaceutical applications.

Conclusions

In this study, the effects of oscillation parameters on system dispersion were evaluated across two commercially available reactors of different scale. Oscillation amplitude was found to have a positive correlation with the dispersion coefficient, with the minimum dispersion coefficient occurring at 1 mm for both systems. This result agrees with those previously presented in the literature. Piston frequency was also evaluated and it was found that optimal operation occurred at 1.5 Hz for the DN6 and 1 Hz for the DN15. However, varying the piston frequency did not have as significant of an impact as the piston amplitude on the dispersion coefficient. Moreover, this result supports Kacker's claim that the mixing parameter Ψ is insufficient in characterizing the oscillatory system.

Prior to this study, distinguishing between pump driven and piston driven flow was omitted in the literature. Piston driven flow leads to an increase in measured dispersion due to the significant back mixing effects that counteract the net flow. While minimal dispersion is desired, one must also keep in mind the inherent benefits of piston oscillations. In liquid reaction systems, vigorous oscillatory mixing improves process kinetics by increasing the propensity of intermolecular interactions. In solid-liquid crystallization systems, the piston oscillations are essential for solid suspension to prevent particle settling and clogging. Therefore, proper OFBC operation is in a pump dominated region which minimizes dispersion, while keeping in mind the oscillatory demands of the system.

Acknowledgements

The authors thank the Department of Education for the funding support through the Graduate Assistance in Areas of National Need (GAANN) program.

Notes

The authors declare no competing financial interest.

References

1. Stonestreet, P., & Harvey, A. P. (2002). A Mixing-Based Design Methodology for Continuous Oscillatory Flow Reactors. *Chemical Engineering Research and Design*, *80*(January), 31–44.
2. Peña, R., & Nagy, Z. K. (2015). Process Intensification through Continuous Spherical Crystallization Using a Two-Stage Mixed Suspension Mixed Product Removal (MSMPR) System. *Crystal Growth and Design*, *15*(9), 4225–4236.
3. Stonestreet, P., & Veeken, P. M. J. V. A. N. D. E. R. (1999). The effects of oscillatory flor and bulk flow components on residence time distribution in baffled tube reactors, *77*.
4. Kacker, R., Regensburg, S. I., & Kramer, H. J. M. (2017). Residence time distribution of dispersed liquid and solid phase in a continuous oscillatory flow baffled crystallizer. *Chemical Engineering Journal*, *317*, 413–423.
5. Dickens, A. W., Mackley, M. R., & Williams, H. R. (1989). Experimental residence time distribution measurements for unsteady flow in baffled tubes. *Chemical Engineering Science*, *44*(7), 1471–1479.
6. Ni, X., & Pereira, N. E. (2000). Parameters Affecting Fluid Dispersion in a Continuous Oscillatory Baffled Tube. *AIChE Journal*, *46*(1), 37–45.
7. McDonough, J. R., Phan, A. N., & Harvey, A. P. (2015). Rapid process development using oscillatory baffled mesoreactors - A state-of-the-art review. *Chemical Engineering Journal*, *265*(1), 110–121.
8. Abbott, M. S. R., Harvey, A. P., Perez, G. V., & Theodorou, M. K. (2013). Biological processing in oscillatory baffled reactors: operation, advantages and potential. *Interface Focus*, *3*(1), 20120036.

9. Ni, X., Jian, H., & Fitch, a. . (2002). Computational fluid dynamic modelling of flow patterns in an oscillatory baffled column. *Chemical Engineering Science*, *57*, 2849–2862.
10. P.N.X. Gough, K. Symes, Experimental flow visualisation in a modified pulsed baffled reactor, J. Chem. Tech. Biotechnol. 69 (1997) 321–328.
11. Ni, X., Brogan, G., Struthers, A., Bennett, D. C., & Wilson, S. F. (1998). A systematic study of the effect of geometrical parameters on mixing time in oscillatory baffled columns. *Chemical Engineering Research and Design*, *76*(A5), 635–642.
12. McGlone, T., Briggs, N. E. B., Clark, C. A., Brown, C. J., Sefcik, J., & Florence, A. J. (2015). Oscillatory Flow Reactors (OFRs) for Continuous Manufacturing and Crystallization. *Organic Process Research and Development*, *19*(9), 1186–1202.
13. Phan, A. N., & Harvey, A. P. (2012). Characterisation of mesoscale oscillatory helical baffled reactor-Experimental approach. *Chemical Engineering Journal*, *180*, 229–236.
14. Ni, X., Mackley, M. R., Harvey, A. P., Stonestreet, P., Baird, M. H. I., & Rama Rao, N. V. (2003). Mixing Through Oscillations and Pulsations—A Guide to Achieving Process Enhancements in the Chemical and Process Industries. *Chemical Engineering Research and Design*, *81*(3), 373–383.
15. Ni, X. W. (1994). Residence Time Distribution Measurements in a Pulsed Baffled Tube Bundle. *Journal of Chemical Technology and Biotechnology*, *59*(3), 213–221.
16. Dickens, A. W., Mackley, M. R., & Williams, H. R. (1989). Experimental residence time distribution measurements for unsteady flow in baffled tubes. *Chemical Engineering Science*, *44*(7), 1471–1479.
17. Smith, K. B. (1999). The Scale-Up of Oscillatory Flow Mixing. *PhD Thesis, University of Cambridge*, (September).

18. Levenspiel, O., & Smith, W. K. (1995). Notes on the diffusion-type model for the longitudinal mixing of fluids in flow. *Chemical Engineering Science*, *50*(24), 3891–3896.

19. Pápai, Z., & Pap, T. L. (2002). Analysis of peak asymmetry in chromatography. *Journal of Chromatography A*, *953*(1–2), 31–38.

20. Wold, S., (2004). Principal Component Analysis. *Chemometrics and Intelligent Laboratory Systems*, *2*, 1–31.

21. Bro, R., & Smilde, A. K. (2014). Principal component analysis. *Analytical Methods*, *6*(9), 2812–2831.

22. Ramkrishna, D. (1974). Stirred pots, tubular reactors, and self-adjoint operators, *29*(6), 1353–1361.

23. Jacobs, C. N., Merchant, W., Jendrassak, M., Limpasuvan, V., Gurka, R., & Hackett, E. E. (2016). Flow scales of influence on the settling velocities of particles with varying characteristics. *PLoS ONE*, *11*(8), 1–20.